Influence of Forming Rate on the Microstructure and Properties of Materials Subjected to Electromagnetic Forming - A Synopsis*

F.-W. Bach, D. Bormann, L. Walden

Institute of Materials Science, Leibniz Universität Hannover, Germany

Abstract

Electromagnetic high speed forming has been known since the 1960's and is successfully used for frictional connexions. In addition to joining, other applications of the process include coining, stamping and cutting. Regarding product quality and manufacturing costs, the process is superior to other methods and yet its utilisation can still be extended.

The synopsis of the material's microstructure and properties owing to electromagnetic forming, which is given by this article, clarifies the processes from a materials science point of view. This will not only represent an academic view point but also provide insight into a potential expansion of the process to other areas of application.

Keywords

Aluminium, Sheet metal Forming, Structure Analysis, High Resolution Microscope, X-ray, Texture, Residual Stress, Strain

1 Introduction

During the past few years various papers have been published in the field of the high speed forming process, however the focus was mainly on the technological aspects of metal forming. But the process is associated with a few effects on the material which are a specific consequence of the electromagnetic forming (EMF). The following conditions are

* *This work is based on the results of FOR 443; the authors would like to thank DFG for its financial support*

examples of the special features of the electromagnetic processing: the forming takes place at high speed, there is no contact with a forming tool if a die is not used and it is associated with a temperature development [1]. All these boundary conditions influence the microstructure and thus specify the specific material properties. Parameters, which characterise the product's behaviour in use, are enormously important because changes in the microstructure entail deviations of the component's properties. Technically pure aluminium shows a strong dependency on forming rate apparent strain hardening. The present investigations are the foundations for a microscopical understanding of the mechanical properties of face centred cubic materials and in particular, provide clarification of the fundamental deformation mechanisms during electromagnetic sheet forming. Examples are mentioned of distortion and premature material failure due to residual stresses. However, residual stresses are not at all invariant and can also be exploited. These exemplary descriptions give information about the material's behaviour and also present possibilities for influencing them provided the physical-chemical properties are known.

2 Metallographic and mechanical investigations

2.1 Microstructural investigations

The material investigated was 1 mm thick sheets of 99.5 % pure aluminium. The work pieces were electromagnetically deep drawn to a depth of 23 mm, figure 1. In order to fully characterise the work piece, different analyses were carried out at various radial points on the sheet. Specimens R4 to R0 were taken along the radius (figure 1 right) for the investigation. Specimen R5 is the initial state of the sheet. The designations internal and external face refer to the tool's coil where the surface of the test piece facing the tool's coil is designated as the internal face and the opposite side of the test piece surface as the external face. The abbreviations RD, TD and ND stand for the rolling direction, transverse direction and normal direction respectively. These designations are retained for all subsequent investigations and are depicted in figure 1.

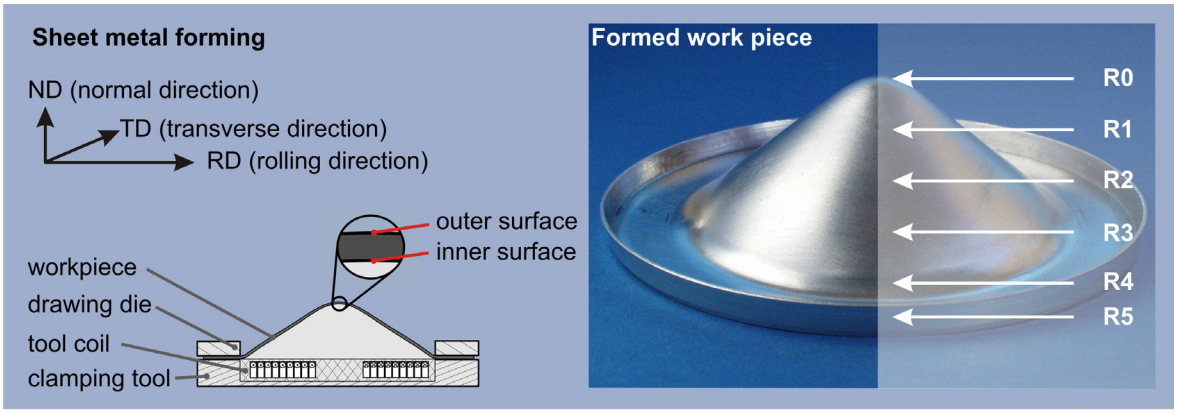

Figure 1: *Electromagnetically formed work piece; regions of interest*

Micrographs of the initial state and the formed work piece are summarised in figure 2. Since no significant differences between the surfaces and the specimen's centre

could be ascertained, the specimen's centre transverse to the rolling direction is depicted here. Analyses of the initial state as well as the formed specimens, which were subjected to variations in their process parameters, are shown in [1]. The deformed microstructure can be represented by two regions: Directly adjacent to the drawing die (R4) and the specimen's centre region (R0). Here, whilst the grain size remains unchanged, the difference in the extent of grain elongation can be metallographically clearly identified.

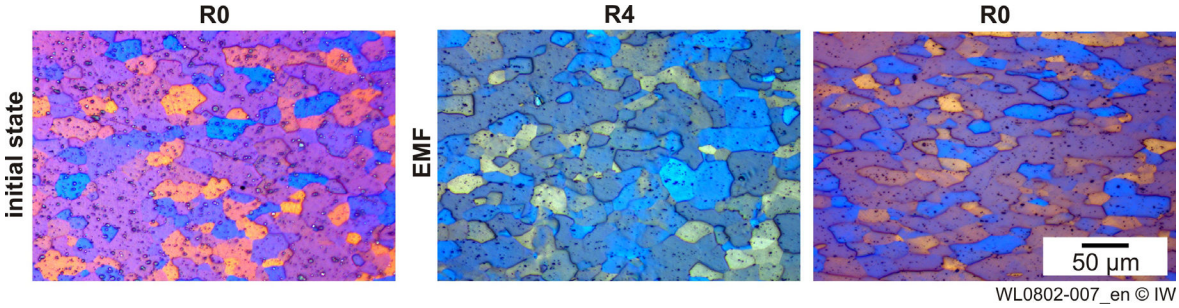

Figure 2: *Micrographs of the initial state and of the drawn work piece in TD*

The quantitative evaluation of the metallographic micrographs was carried out according to the planimetric procedure using the SIS image processing software in agreement with ASTM E112 and DIN 50601. The computing algorithm is based on a grain boundary reconstruction and is insensitive to deleterious inclusions and etching effects. The results of the grain size and grain elongation evaluation can be seen in figure 3.

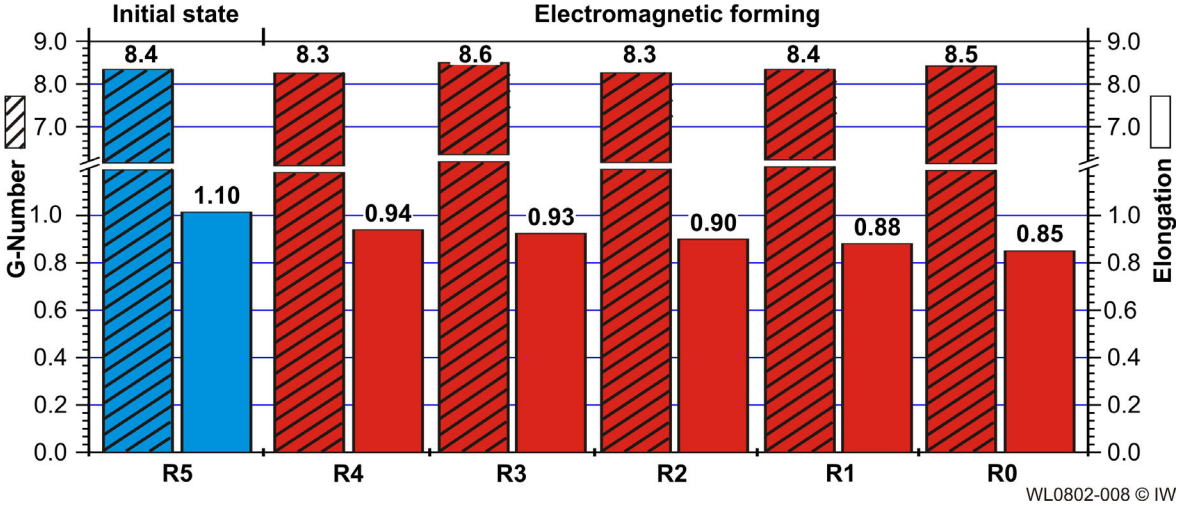

Figure 3: *Grain size and grain elongation in the initial state and in the formed work piece*

The grain size is relatively homogenous with mean values of G=8.4 ± 0.1 for the initial state and for the deformed specimens respectively, implying a grain diameter of approx. 18 µm. The grain elongation is computed as the ratio of the vertical to horizontal grain sizes and is 1.01 in the initial state (R5). For the formed work piece, the ratio continuously increases from 0.94 in the flange (R4) region up to 0.85 at the specimen's centre (R0).

2.2 Sheet metal thickness and micro hardness distribution

The wall thickness was measured along the specimen's radius in the RD and TD. No significant difference could be ascertained by comparing the RD with the TD results (figure 4 left). The continuous decrease in wall thickness along the radius towards the specimen's centre amounts to 974 ± 12 µm at the edge and 660 ± 10 µm at the specimen's centre (R0).

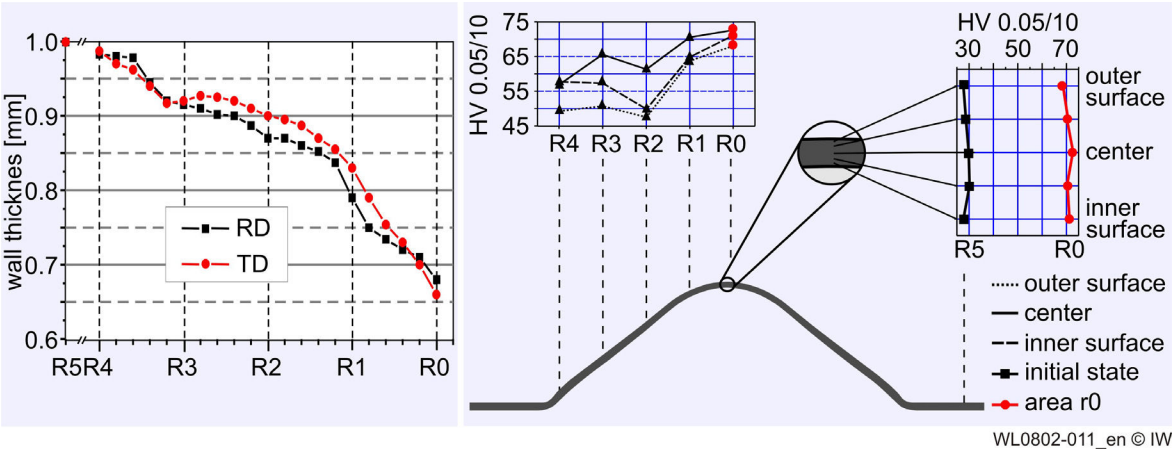

Figure 4: *Sheet metal thickness and micro hardness in the initial state (R5) and in the formed work piece (R4-R0)*

The hardness variations were measured in the sheet thickness direction (ND) in its initial state to ascertain the existing differences between the edge and the centre-line and to be able to compare these with the values from the deformed specimens. The hardness values determined show no significant differences between the external and internal faces and the specimen's centre. The mean microhardness is 29 ± 2 HV 0.5/10. A significantly higher microhardness is shown in the direction of the specimen's centre of the formed work piece. In the region R4, the microhardness has a value of 54 ± 3 HV 0.5/10 and in the region R0, a value of 71 ± 2 HV 0.5/10 (figure 4 right).

The qualitative and quantitative metallographic investigations show a microstructure with uniform grain sizes and differences in grain elongation, which increase towards the work piece's centre. The wall thickness continuously decreases towards the work piece centre-line and in this region the sheet thickness is 34 % of its initial value. Simultaneously, an increase in microhardness is measured along the specimen radius, which rises from 86 % at the edge region to 145 % at the specimen's centre.

3 Transmission electron microscopy analysis

In order to gain a comprehensive understanding of the deformation mechanisms, investigations using a transmission electron microscope (TEM) were necessary. General and detailed micrographs were taken with different magnifications at the individual sampling locations from figure 1.

Two regions are depicted in figure 5 which represent the initial state of the material. In the left portion of the figure 5, the grain boundaries of a total of five grains can be seen.

However due to their size, a whole grain cannot be recorded using the TEM. Owing to the different crystallographic orientations, etching effects occur during the specimen preparation and, as a result, geometrically arranged patterns in the microstructure can be seen. In the micrograph, several precipitates as well as isolated dislocations can also be seen. In the right portion of the figure 5, a row of dislocations can be detected next to individual dislocations. In general, the dislocation density is very low, indicating heat treatment during the sheet manufacture.

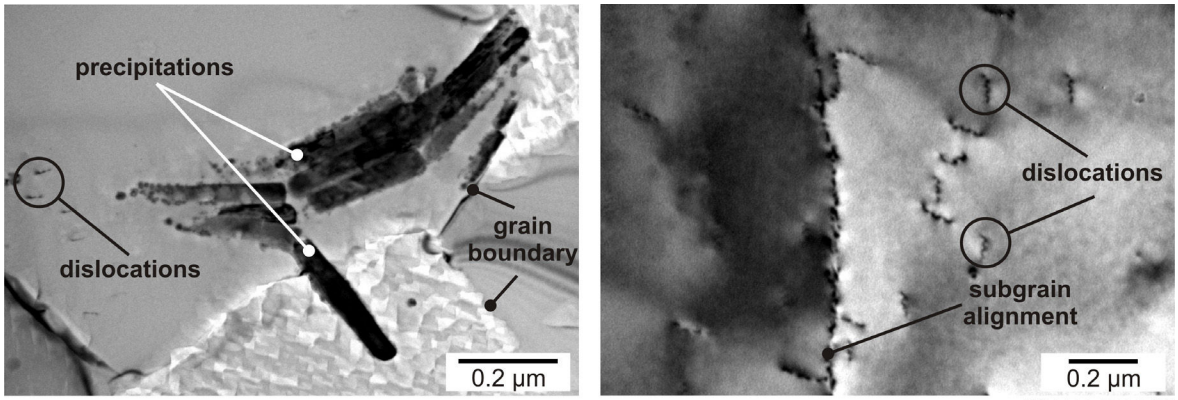

Figure 5: *Microstructure of the initial state (R5)*

The microstructures of the formed work piece from the flange region (R4) are shown in figure 6. The microstructure can be characterised as follows: In comparison to the initial state, there are regions which exhibit more individual dislocations, but the dislocation density is generally low (figure 6 left); here and there dislocation tangles and arrangements of dislocations can be observed (figure 6 right).

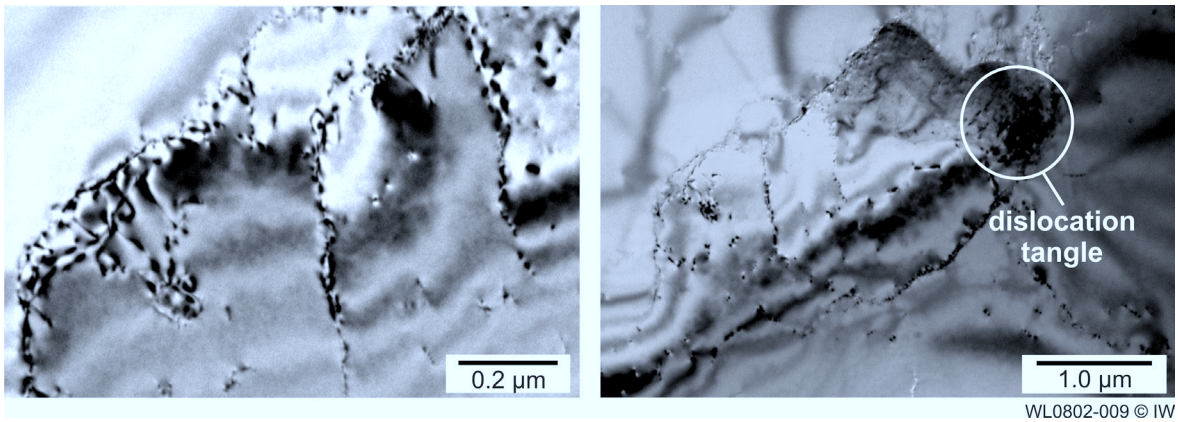

Figure 6: *Microstructure of the formed work piece, R4 region*

The microstructure from the specimen's centre is depicted in figure 7. Here, a pronounced cell structure can be seen with thin cell walls and different cell sizes. In many places, dislocation networks are still detectable; however, the cell walls already indicate sub-grain boundary character. The differences in contrast are an indication of the distinct orientations between the delineated regions (figure 7 left). This signifies that, in this case, sub-grains are involved.

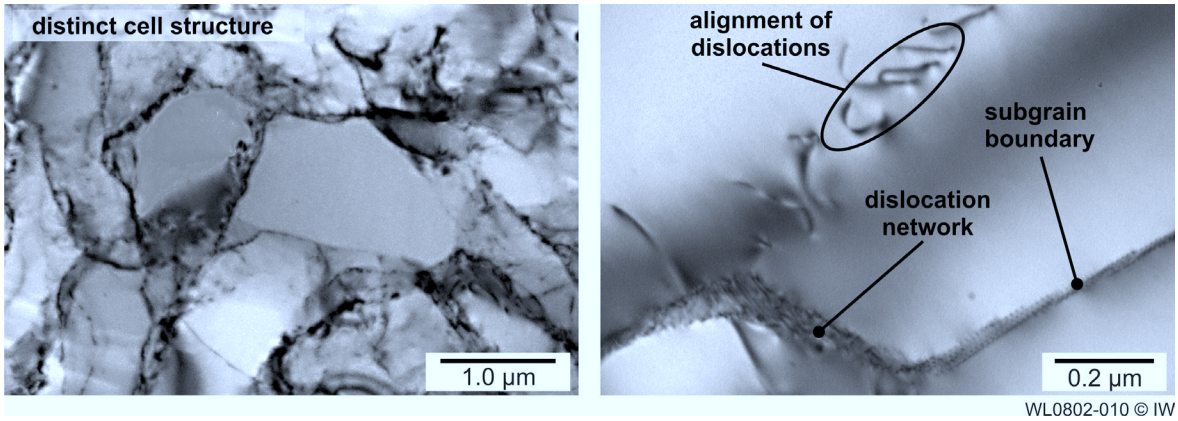

Figure 7: *Microstructure of the formed work piece, R0 region*

The TEM investigations of the forming process considered here show typical features of deformation at low temperatures; that is, temperatures below 0.4 T_s (T_s: melting point). According to the classification of Honeycombe, the electromagnetically formed specimen, depending on the level of loading, is assigned to the range I to III [2].

The TEM investigations unambiguously show that this involves cold forming. Traditionally, as is known from the theory of crystal plasticity, the dislocation density initially increases followed by observations of dislocation localisations which form tangles into cell structures with different cell wall thicknesses until sub-grains finally emerge. It is novel that all these stages of microstructural development can be observed along the radius within the work piece. The flange region exhibits a comparatively low dislocation density which indicates a smaller degree of deformation. The microstructure, depending on the degree of deformation, is evidently "frozen" into the sequential stages owing to the high deformation rate. As the degree of deformation increases, the dislocation evolution progresses until a sub-grain structure emerges in the work piece. By means of this distinct deformation history in the work piece, the differences in grain elongation and microhardness can be explained.

4 X-Ray analysis

4.1 Texture

To determine the macro-texture, X-ray diffraction techniques were employed. The orientation distribution function (ODF) was computed according to Bunge. The influences of the electromagnetic forming, related to the degree of deformation, are not uniform. Since the forming conditions can be expressed by two starkly contrasting regions (R4 and R0), these are graphically depicted in the following together with the initial state (R5).

The legend for the pole figure distribution is shown in figure 8 below left. From the sheet's pole figure in the initial state and the computed ODF, a texture becomes visible which corresponds to the ideal orientation (figure 8 above left and figure 9 left). In this case, it involves the (001) [100]-orientation or the cube alignment.

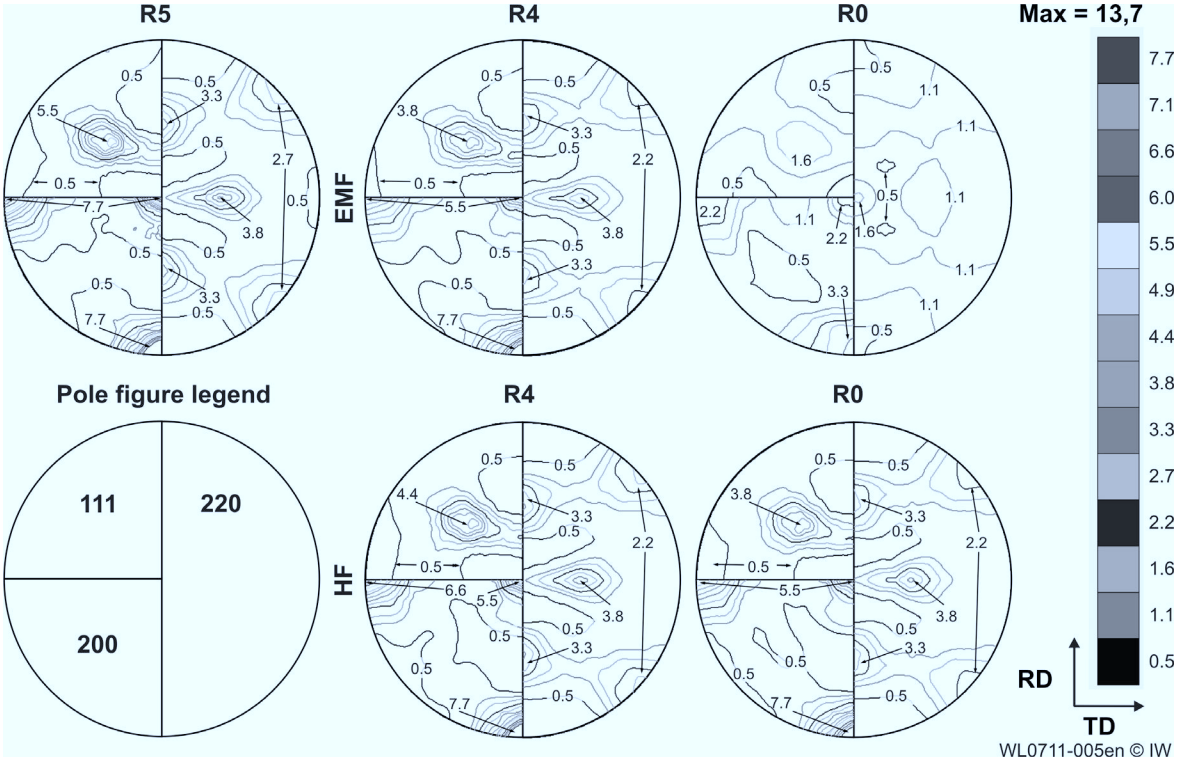

Figure 8: *Pole figures for the initial state (R5) and for the formed work pieces (R4 and R0)*

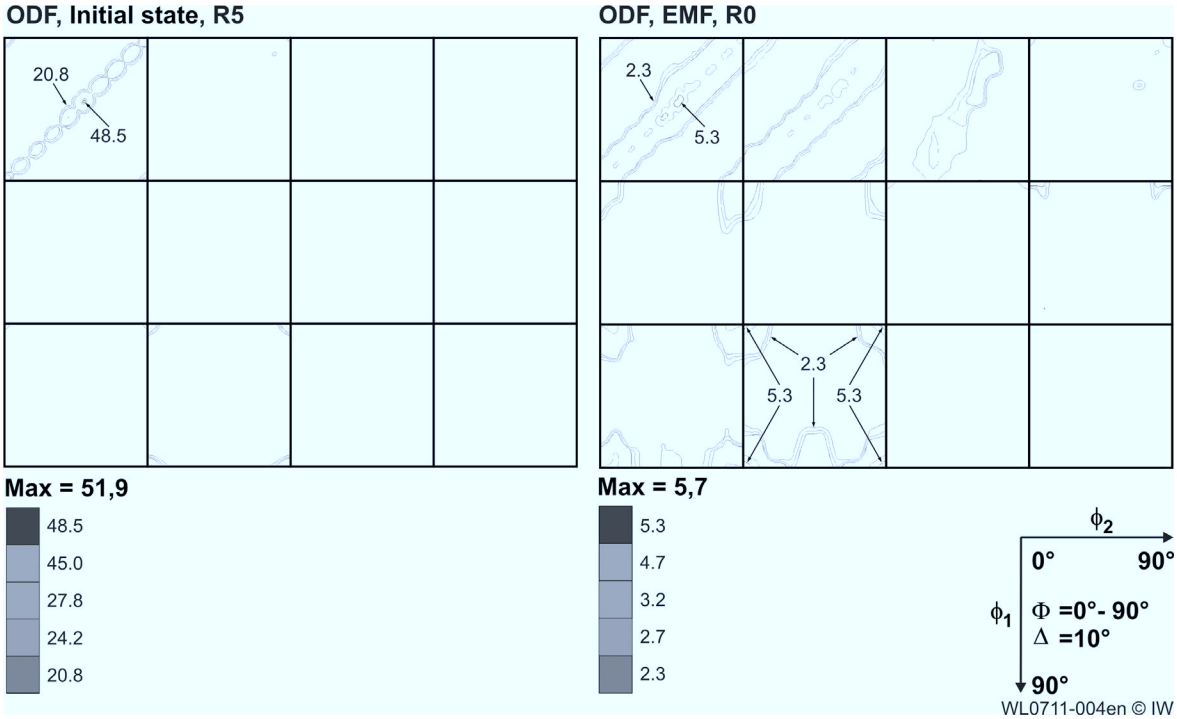

Figure 9: *ODF for the initial state (R5) and for the formed work piece (R0)*

The pole figures for the EMF specimen are depicted in figure 9 above centre and right. A reduction of the texture can be observed (see table 1) along the specimen radius from the drawing die to the cup centre. The reason for this is the sub-grain formation (see

section 3), which is discontinued by the advanced microstructural development at high deformation rates. Also, the texture type is modified with increasing degrees of deformation. Besides the attenuation of the existing cube texture, a second orientation is indicated. Using the 220 pole figure (figure 8 above right) as an example, it is clear that the four fold symmetry, recognisable from the maximum packing density along the periphery as well as both paired maximums along the RD or TD, is almost eliminated. Instead of this, a new, weakly pronounced texture component is added. To describe the new texture, the ideal orientations (0-11) [-111] and (0-11) [-211] can be taken into consideration. Owing to the attenuation of the intensity, this orientation can not quite be uniquely determined. As a comparison, hydraulically formed (HF) specimens were also investigated (figure 8 below centre and right). The measured regions of the work piece have the same nomenclature as that for the EMF specimens, and are depicted in figure 10 left. Here, an attenuation of the existing texture along the radius is also found. However, this is not as clearly pronounced as that for the EMF and no further components are observed.

Since the computation of the ODF did not result in a large difference in the function's graphical representation, the representation of the initial state is typified by the regions R5 and R4. An exception to this is the region R0 for the EMF with the highest degree of deformation (figure 9 right) for which the new component can also be seen in the ODF.

Clarification of the material's quantitative texturing is given by the maximum value of the measured or computed intensity as well as the values of the corresponding ODF's, which are summarised in the **Table 1** .

Area	Initial state, R5	EMF, R4	HF, R4	EMF, R=	HF, R0
Max. intensity	13.7	10.7	12.4	3.7	10.4
Reduction in %	-	21.9	9.5	73.0	24.0
Max. ODF- Value	51.9	30.6	42.1	5.7	28.2
Reduction in %	-	41.0	18.9	89.0	45.6

***Table 1**: Values of the intensity and the ODF*

The results of the investigations using the X-ray diffraction technique show that a cubic texture existing in the material is, with over 90 % reduction, almost eliminated. Only in regions of the highest degree of deformation (work piece centre) can a new, very weakly pronounced texture component be ascertained. The texture reduction guarantees almost isotropic material behaviour, whereas the texture is only attenuated for quasistatic processes.

4.2 Residual stress

Similar to the texture investigations (see section 4.1), the specimens were measured both in the rolling direction and along the specimen radius. The specimens were mounted such that the psi-tilting plane and the rolling direction were aligned parallel to each other. The evaluation of the measured results was carried out using the sin²-psi-procedure.

In the initial state, slight compressive residual stresses were measured (figure 10). This is a case of type I residual stresses and especially of thermal residual stresses which originated during the sheet manufacture from shrinkage effects as a result of thermal influences or heat treatment. In the formed region of the EMF, the residual stress magnitudes are both tensile as well as compressive. It can be seen that the highest tensile residual stress values occur in the region of the drawing die. The reason for this is the transition from the deep-draw loading, where insufficient continuous flowing of the material occurs, into stretch-form loading. In the work piece centre, marginally reduced tensile residual stresses were measured. Apart from the usual tensile material stresses, alternating stresses are superposed owing to the wave like movements of the sheet during forming. In these regions, material failure occurs at higher degrees of deformation, as can be expected from the values of the residual stresses. Compressive residual stresses are observed along the radius. Here, the analysis was also augmented with comparative investigations of a HF work piece. In the HF, a relatively high loading of the material in the tensile direction is observed. Along the radius, the residual stresses are continuously relieved by up to 30 %, but are retained in areas of tensile residual stresses. For both forming methods as well as their hybrids, types II or III residual stresses are involved.

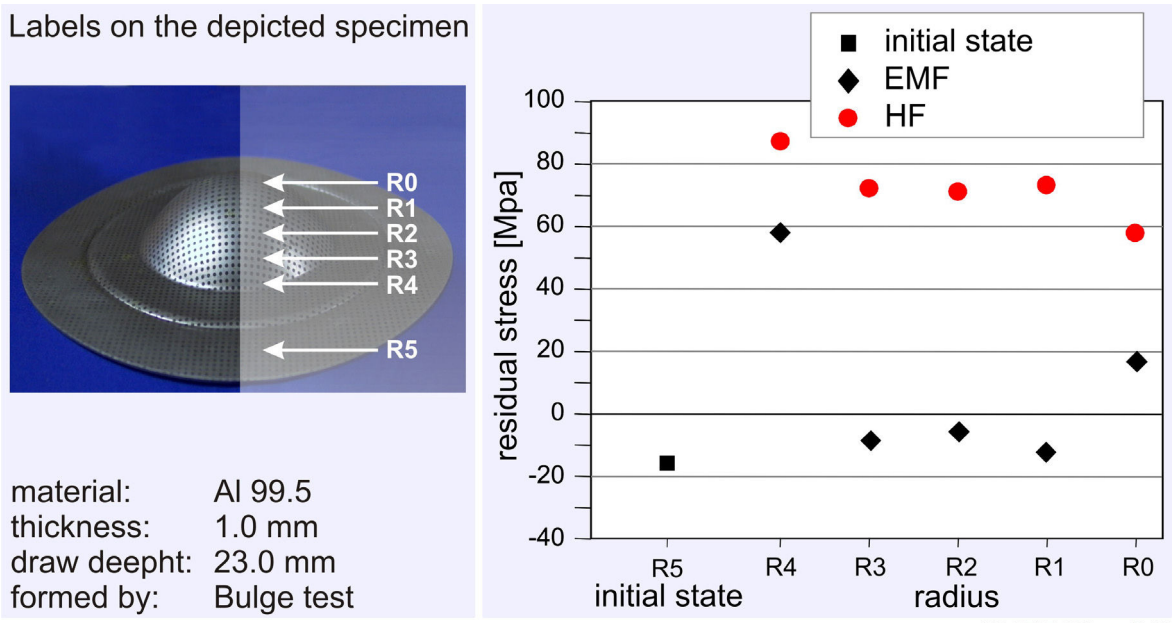

Figure 10: *Residual stress in the initial state (R5) and in the formed work piece (R4-R0)*

The measured residual stresses shed light on the failure behaviour of the sheet as a consequence of forming. Electromagnetically formed specimens have an advantageous residual stress state which lies in the region of compressive residual stresses and has a positive effect on, for example, the surface properties such as corrosion and crack formation. Tensile residual stresses were measured at only two locations: Adjacent to the drawing die (in the deep-drawing region) and in the work piece centre where a significant reduction of material occurred. In this region, material failure takes place at higher loading.

5 Conclusions

The aim of the investigations presented here is to provide an overview of electromagnetic forming, a dynamic forming process using strain rates of up to 10,000 s 1, with respect to the influences on the material.

In conclusion, it is essential to remember that the microstructural differences between conventional and electromagnetic forming processes only result from the deformation rate and the degree of deformation. From the investigations presented here, it can be derived that the changes in the work piece properties can be primarily attributed to the microstructural processes within the grain, in particular sub-grain formation. With regard to component applications, it must be taken into consideration that the deformed material exhibits almost isotropic behaviour with significantly higher microhardness which is not based on residual stresses caused by the forming, but on sub-grain formation. Possible material failure must be diagnosed or predicted, as the case may be, using appraisals of the residual stress state.

Subsequent to the forming, different microstructural analyses show a fine grained microstructure which could be clarified using a transmission electron microscope [3]. Employing a fine grained structure is an efficient method to improve the mechanical properties of materials (s. procedures like ECAP [4]). The work hardening gained by using this process creates totally new possible applications for the material. This grain refinement takes place by the formation of subgrains as a result of electromagnetic forming. These effects are due to a type of dynamic recrystallisation, which take place during the process.

The synopsis of the material's microstructure and properties owing to electromagnetic forming, which is given by this article, clarifies the processes from a materials science point of view. This will not only represent an academic view point but also provide insight into a potential expansion of the process to other areas of application.

References

[1] *Bach, Fr.-W.; Rodman, M.; Rossberg, A.; Weber, J.; Walden, L.:* Verhalten von Aluminiumwerkstoffen bei der elektromagnetischen Blechumformung. 2. Kolloquium elektromagnetische Umformung, Dortmund 2003, p. 11-19,

[2] *Honeycombe, R.:* The plastic deformation of metals. Edward Arnold Ltd. London, 2. ed., 1984

[3] *Bach, Fr.-W.; Walden L.:* Mikrostruktur und mechanische Eigenschaften von Kupferblech. Unter der Einwirkung von elektromagnetischen Kräften, ZWF, vol. 100, iss. 7/8, Hanser Verlag, p. 430-434, 2005

[4] *Hellmig, R. J.; Estrin, Y.:* Ultrafeinkörnige Kupferwerkstoffe - ein Weg zu verbesserten Eigenschaften. Metall, vol. 60 iss. 11, p. 702-704, 2006